INSTRUMENTS AND EXPERIMENTAL TECHNIQUES, 2025, No. 1

GENERAL EXPERIMENTAL TECHNIQUE

3D DESIGN OF AN ALL-METAL WAVEGUIDE CO2 LASER WITH TRANSVERSE HF EXCITATION

© 2025 V. A. Stepanov[a,*], E. N. Moos[a], R. S. Rumyantsev[a], A. I. Kudyukin[a], K. I. Bobrovsky[b], A. Ya. Payurov[c]

[a]*Ryazan State University named after S.A. Yesenin Russia, Ryazan*

[b]*LLC "Vacuum Technologies" Russia, Ryazan*

[c]*JSC "Plasma" Russia, Ryazan*

**e-mail: vl.stepanov@365.rsu.edu.ru*

Received February 13, 2024

Revised June 24, 2024

Accepted November 29, 2024

Abstract. The work is devoted to 3D design of a new device at the development stage – an all-metal waveguide CO2 laser (elements and the entire device) using domestic precision aluminum profiles. A 3D view of individual units and the entire laser is shown. Air and water cooling schemes, assembly and sealing technology of the CO2 laser using laser (plasma) welding and adhesive joints are described, ensuring high quality and reliability of the device.

DOI: 10.31857/S00328162250122e2

1. INTRODUCTION

Gas discharge CO_2-lasers are one of the most representative classes of lasers. High efficiency, power range, high monochromaticity of radiation ensures the locality of their impact. At the same time, the ability of CO_2-lasers operate in pulsed, pulse-periodic and continuous generation modes. These devices are indispensable in physical research and in materials processing technology [1, 2].

Continuous expansion of application areas and competition force specialists of leading companies to develop new and continuously improve already created models. As a result, compact all-metal devices have taken the leading position in the industrial products market today. Especially

notable is the waveguide version with transverse high-frequency excitation. The designs of these lasers use precision rolled aluminum alloys, modern methods of shaping, and advanced technologies for high-hermetic connections [3-5].

The relevance of the work is due to extensive research on all-metal waveguide CO_2-laser. Its design is based on domestic precision aluminum profiles and 3D design methods [6, 7].

2. 3D DESIGN OF COMPONENTS AND CONSTRUCTION OF ALL-METAL WAVEGUIDE CO_2-LASER

3D modeling is the process of creating a three-dimensional model of an object and developing a visual volumetric image of the desired object. With the help of three-dimensional graphics, it is possible to create an exact copy of a specific item and develop a new, often difficult to imagine construction.

The main advantage and benefit of 3D modeling is visibility and the possibility of simultaneous parallel design. This ensures automatic coordination of changes and modifications to both components and the entire device. In addition, it has become possible to calculate thermal and strength performance characteristics at all stages of device development and manufacturing. Modern technological processing centers and computer numerical control machines significantly reduce the manufacturing time of the product and the time interval from idea to finished product.

The design development was carried out in the KOMPAS-15 software environment.

Figure 1 shows a variant of a Z-shaped discharge structure formed by two channel electrodes made of aluminum alloy AD31T. The waveguide Z-shaped channel is obtained by milling corresponding semi-cylindrical grooves on the external surface of these channels and subsequent symmetrical assembly. The channel diameter is approximately 3 mm. To reduce waveguide losses at the working wavelengths of the CO_2-laser, the electrode surface is coated with aluminum oxide (α-Al_2O_3).

Fig. 1. Variant of a Z-shaped discharge structure

A channel of this shape allows for reducing the overall dimensions while maintaining the same laser radiation power per unit length. However, this design requires additional turning mirrors with adjustable positioning.

Maintaining the discharge in the working channel requires preventing its development in the non-working gap between the electrodes. The condition for this is as follows: the value of the

interelectrode gap (approximately 0.5 mm) is significantly smaller than the diameter of the working channel (about 3 mm). At the working pressure of the gas mixture in the working channel, discharge in gaps less than 0.5 mm is impossible due to the slow formation of the necessary near-electrode layers. The gap size and its adjustment are ensured by installing additional ceramic fixators at the ends and in the middle of the discharge structure.

Grooves approximately 0.5 mm deep are milled on the outer surface of the electrodes. Ceramic aluminum nitride (AlN) plates with a thickness of 1 mm are placed in these grooves to insulate the housing and the discharge structure. Matching inductance coils made of copper wire with a diameter of 1.5 mm (approximately 23 pieces) are installed in the inner cavity of each channel electrode. Additional fixation of the electrodes and increased overall rigidity of the discharge unit (armature block) are provided by ties. In the middle of the external surface of the electrodes, there are two threaded M4 holes for current leads that supply high-frequency power. The electrodes are connected with studs, with ceramic washers and an interelectrode gap regulator fixator added.

The advantage of this emitter design is in the use of aluminum alloy profiles. The chosen symmetrical cross-section of the laser housing provides resistance to external influences. The compactness of the laser as a whole and the reliability of its excitation are achieved by the possibility of combining the RF excitation source and the emitter. During assembly, careful control of the hermetic sealing of the component connections is required. It should be taken into account that the device can operate at elevated temperature conditions, especially with air cooling. This is required when creating heat sinks. The necessary degree of insulation is provided by reducing non-working gaps, in which discharge occurrence is difficult, as well as by alundizing (oxidizing) the contacting surfaces and thin ceramic washers.

Cooling is carried out by two aluminum heat sink plates with channels for water flow (Fig. 2).

Fig. 2. Assembled discharge structure 3D and housing (box)

The heat sinks have a symmetrical shape. The channels for cooling fluid flow are also symmetrical. The bends in the channels contribute to the emergence of turbulent fluid flow and heat dissipation efficiency (Fig. 3).

Fig. 3. 3D model and 2D drawing of the liquid cooling heat sink

The adjustment flanges are two plates with openings for mirrors, evacuation stems and fasteners (Fig. 4). The flanges made of AD31T alloy have a parallelepiped shape and possess high bending rigidity and great mechanical strength.

Fig. 4. Flanges with adjustment units (2D and 3D images)

The RF driver is a self-oscillator with four transistors (Fig. 5) with a nominal frequency of 81.36 MHz. It performs RF pumping of the laser active medium. MOSFET transistors MRF150 with an operating frequency range of 30-150 MHz, current load of 16 A, and maximum output power up to 150 W were used as power high-frequency transistors. The self-oscillator has a symmetrical output and is connected to two current leads of the emitter. Adjustment of the average pumping power is carried out using a pulse-width modulator (PWM) for the power transistors' supply (Fig. 5).

Fig. 5. 3D model of a high-frequency driver

The discharge structure-waveguide is placed inside the box. AlN (aluminum nitride) insulators are installed in the slots of the discharge structure. They serve as electrical isolation between the discharge structure and the box (Fig. 6).

Fig. 6. Box with discharge structure

The box and heat sink plates are connected with M6 studs with rigid fixation of the discharge structure position inside the box. M5 screws connect the flanges assembled with alignment units, mirrors, and a valve for evacuation/filling. At the junction of the flanges and the box, there is a rubber seal for hermetic sealing of the volume (Fig. 7). The HF driver is installed on the upper heat sink.

After assembly, the operations of evacuation, annealing, and filling the laser working volume with gas mixture follow. Then the device is trained (Section 3).

Fig. 7. Sealed box with optical system

3. THERMAL MODES

Depending on the purpose, waveguide CO_2-lasers can be operated in an ambient temperature range from -50 °C to +55 °C, provided that their thermal operating modes are ensured.

According to the method of heat dissipation from the discharge, the devices are divided into emitters with air (A) and liquid (L) cooling. In the first case, cooling occurs due to natural or forced air convection on radiators with an extended surface (longitudinal or transverse fins, as well as multi-pin options).

Taking into account the symmetry of the emitter, heat fluxes are considered only in one of the quarters (one quadrant) of the cross-section (Fig. 4). Heat exchange from the ends of the emitter is neglected. In this case, the initial amount of heat generation will be about 225 W. The air-cooled heat sink is a set of stamped plates made of aluminum alloy. They are fixed on the outer surface of the housing using a thermally conductive paste such as KPT-8. The outer surface of the plates is a finned

heat sink: fin height 26 mm, distance between fins 6.3 mm, number of fins 15, material - aluminum alloy AD 31 with thermal conductivity 188 W/(m·K) (Fig. 8).

Fig. 8. Direction of Heat Flow

The efficiency of this radiator is achieved by forced air flow with a velocity of V = 6.5 m/s at atmospheric pressure and temperature of 20 °C. The cooling radiator for the laser emitter is a radiator profile made of aluminum alloy AD31T with thermal conductivity of 188 W/(m·K).

For effective cooling, the coverage area is increased. This is provided by fins with heights from 20 mm to 35 mm. With liquid (water) cooling, the radiators have appropriate channels. When the laser power is about 40-45 W, increased heat dissipation is required. Therefore, liquid cooling is used in this device. When evaluating the efficiency of heat dissipation in the emitter, it is necessary to consider the conditions of heat exchange on the contacting surfaces with temperature differentials. For a radiation power of 40-45 W, the active discharge length should be about 111 cm, with a real efficiency of 10%, the discharge power is approximately 450 W. Taking into account the RF source, the total heat release reaches approximately 900 W.

Let's consider the heat flows, taking into account the symmetry of the emitter, only in one of the four quarters (one quadrant) of the cross-section (Fig. 9).

Fig. 9. Direction of heat flows with liquid cooling

In the cooling channels, forced convective heat exchange occurs during fluid movement. The heat flow is proportional to the wall surface area and the temperature difference between the fluid and the wall (temperature head):

$$W = \alpha\ S\ \Delta t. \qquad (1)$$

Various factors influence the heat transfer coefficient α. These include the physical properties of the fluid, its flow rate, the geometry and quality of the cooling channel surface. This determines the laminar, transitional, or turbulent fluid flow regime. The flow rate and shapes of the cooling channel set the turbulent fluid flow regime, which increases the efficiency of heat exchange. The nature of the fluid flow is determined by the Reynolds number

$$\mathrm{Re} = \frac{4\ V}{\pi\ d\ \nu}, \qquad (2)$$

where V [m^3/s] – volumetric fluid flow rate, d [m] – diameter of the cooling channel, ν [m^2/s] – kinematic viscosity of the fluid.

At Re < 2200, the fluid flow regime in a pipe is laminar. For Re from $2.2 \cdot 10^3$ to $1 \cdot 10^4$ a transitional regime is realized, and at Re > $1 \cdot 10^4$ – turbulent.

The heat transfer coefficient α in forced fluid motion is calculated based on the relationships

between the Nusselt Nu_f, Reynolds Re_f and Prandtl Pr_f criteria.

4. TECHNOLOGICAL ASPECTS OF SEALING AND THERMAL VACUUM TREATMENT OF ALL-METAL WAVEGUIDE CO_2-LASER

Conventional joining methods in laser construction provide extremely low gas permeability and outgassing. In recent years, various types of seals and adhesive joints have been actively used for these purposes, due to the emergence of new materials and modern technologies.

Traditional methods of sealing the construction of gas-discharge CO_2-lasers are various types of welding and soldering. Until recently, adhesive joints were primarily used for sealing optical elements. This is, first of all, the film adhesive PCS-171 (TU 6-06-20-88), which is obtained from an alcohol-water solution of polyamide resin 6/66/610-1, adhesive PFE-2/10, epoxy resin ED-20, dicyandiamide, phosphonitrilanilide and aminopropyltriethoxysilane (coupling agent AGM-9).

Metals (steel and its alloys, aluminum and its alloys, duralumin, gold, silver, etc.) are glued with non-metallic materials (ceramics, quartz, glass, carbon fiber, polyamides, etc.) in the temperature range from 120 °C to 240 °C, pressure from 0.05 to 4.5 MPa (from 0.5 to 45 kgf/cm ^{2}) with exposure from 20 s to 5 h.

These adhesive joints are characterized by high strength of the adhesive joint, high electrical insulation properties, good dielectric properties, as well as low gas permeability and outgassing. The operating temperature range is from -60 °C to +150 °C, briefly up to +200 °C [8, 9]. Effective use of this type of adhesive and adhesives in general requires preparation of the surfaces to be joined. It is usually carried out in two stages.

An important distinctive feature of modern designs of all-metal CO_2-lasers is the widespread use of seals made from various materials, particularly from Viton and indium. Let's examine their characteristics in more detail.

From a chemical perspective, the synthetic rubber-like material (elastomer) Viton is a linear copolymer of vinylidene fluoride and hexafluoropropylene. This material is available as gaskets with round or flat cross-sections in various shapes [10].

When sealing modern all-metal structures, seals made of highly plastic metals are used. In particular, these are gaskets made of indium or its alloys with other metals. Such seals can be almost infinitely deformed under pressure, as they do not harden during processing. This is extremely useful for dismountable or unsoldered devices operating at temperatures below the melting point of indium [11]. Additionally, it is resistant to strong alkaline solutions.

The general structural scheme for manufacturing a gas-discharge CO_2-laser includes operations of metal processing, cleaning and heat treatment of parts, seal gaskets, assembly and control of assembly operations, mirror alignment, as well as matching the emitter with the RF generator. The finishing operations are thermal vacuum processing, training in the working gas mixture, final assembly, adjustment, and measurement of the laser parameters as a whole.

The presence of hydrogen, water, organic impurities, including oil vapors in the gas medium reduces the radiation power and affects the durability of the CO_2-laser. Therefore, at the assembly stage, all parts are thoroughly degreased in trichloroethylene and degassed in vacuum. This ensures effective removal of hydrogen from the volume of the parts. If the construction material is aluminum, then in the presence of atomic and molecular oxygen in the discharge, an oxide film is formed. Irreversible removal of oxygen from the medium occurs, which shifts the equilibrium of the dissociation reaction to the right. To prevent this, the discharge structure parts undergo a two-stage treatment.

In the first stage, the parts are mounted on the fixture, soldered into glass bulbs, annealed in vacuum, and then oxidized in oxygen at a temperature of 300 ºC for 3 hours. The thickness of the oxide film after annealing and oxidation is 0.3-0.8 μm, which is monitored with a MII-4 microinterferometer.

Thermal vacuum treatment includes pumping, degassing in a furnace, and training in a discharge mixture of working gases. The next stage is training in the discharge of the working gas mixture. It consists of CO_2, nitrogen, helium, xenon in a ratio of 1:1:4:0.25; the training takes place in a cyclic mode - 4 times for 60 minutes with pumping and replacement of the filling. Training in the discharge ensures saturation of the surface layers of the fixture elements with working gases and initial processing of the electrode surfaces. However, this does not ensure the operability of the emitter for a long period of time [3]. The degradation of the working mixture is caused by the dissociation of CO_2 molecules. The degree of dissociation increases over time, which is associated with the gradual irreversible loss of oxygen formed during dissociation.

To reduce the rate of oxygen loss or compensate for these losses, various methods are used - both passive and active. Passive methods include the use of additional volume.

More effective for reducing oxygen losses, as shown by mass spectrometric studies, is the passivation of the surface during long-term (about 100 hours) training of the active element in the discharge of the channel's working mixture. It leads to a decrease in oxygen losses. At the same time, there is an intensive saturation of the discharge channel walls with components of the working mixture and relatively shallow oxidation of metal surfaces. Such passivation, combined with the deposition of

an Al_2O_3 film, allows increasing the durability of the CO_2-laser several times (up to 5000 hours or more) [3].

5. ENERGY CHARACTERISTICS

The main laser parameters typically include radiation power, its time dependence, beam diameter and divergence of laser radiation, polarization, spectral composition (wavelength, number of frequencies, etc.). Devices can operate in both continuous and pulsed (periodic) modes, therefore measuring these characteristics requires the use of measurement equipment with different response speeds. Extending conventional optical measurement methods to such small time frames and extremely high flux densities requires both improvement and development of old methods, as well as creation of new measurement techniques.

More sophisticated laser parameters include the specifics of the resonator mode spectrum, gain, noise, and modulation capabilities. Measurement of internal and external laser parameters is carried out using signal, power, and energy sensors [1].

When measuring beam divergence using the two-section method, the laser beam is directed to the input device (of the radiation beam power density distribution meter), and the signal from it is fed to a two-coordinate recorder.

To measure the basic energy and spectral characteristics of the assembled experimental sample, a measuring system was created, the block diagram of which is shown in Fig. 10.

Fig. 10. Block diagram of the experimental setup for measuring energy and spectral characteristics of laser radiation

Radiation from the laser passes through the attenuator *4* and goes either to the power meter *5* , or to the radiation beam power density distribution meter *7* , or to the PAS.

When measuring the beam divergence by the two-section method, the laser beam is directed to the input of device *7* (beam power density distribution meter), the signal from which is fed to a two-coordinate recorder *6* . The divergence is estimated based on the measurement results of two laser beam diameters at distances of 500 and 1000 mm using the formula

$$\Theta_P = \frac{d_1 - d_2}{\Delta L}, \qquad (3)$$

where Θ_P [rad] - beam divergence, ΔL [mm] - distance between two sections where diameters are measured, d_1 [mm] - beam diameter measured in the first section, d_2 [mm] - beam diameter measured in the second section.

Parameters are measured at the 0.5 maximum level. On the recorded curve, points at the level of 0.5 of the maximum value are marked and connected with a straight line segment of length Δx_1, Δx_2 [mm] for the first and second sections respectively. The beam diameters are determined as follows:

$$d_1 = k \cdot \Delta x_1 \,,\; d_2 = k \cdot \Delta x_2 \,, \tag{4}$$

where d_1, d_2 [mm] - beam diameters at the 0.5 $A_{\max}$ level for the first and second sections respectively, k - scale factor determined by the technical characteristics of the scanning device and plotter (k = 0.18).

Diagrams explaining the principles of measuring beam divergence and diameter are shown in Fig. 7, 8.

Power measurements were conducted in the forced mode of the oscillator with 70% PWM, with an output mirror having a transmission coefficient of 30%, and at a gas mixture pressure of 80 mm Hg. At 70% PWM (Power Width Modulation - a process of power control by periodically turning the device on and off) the radiation power was 22 W (Fig. 11-13) .

Fig. 11. Scheme for measuring beam divergence

Fig. 12. Scheme for measuring laser beam diameter by radial distribution of radiation density

Fig. 13. Dependence of radiation power on PWM level

The measurement of radiation power was carried out in a non-forced oscillator mode with a pulse power of about 500 W and at gas mixture pressures of 70, 80, 85, 90, and 100 Torr (see diagram). A gas mixture with a composition of 6 CO_2, 3.75 N_2, 25 He, 2 Xe was used. The optimal pressure value in the prototype laser was 80 mm Hg, which is typical for waveguide lasers with a channel diameter of about 3 mm and close to the invariant pd = 250, where p [mm Hg] is pressure, d [mm] is the discharge channel diameter (Fig. 14) .

Fig. 14. Dependence of radiation power on gas mixture pressure

The laser beam parameters were obtained using a Pirocam-3 meter. The measurement results have some deviation from theory. The meter also determined the beam astigmatism (Z_y Z Z_x)/ Z_{rr} = 7.6%, waist asymmetry 2 Wy /2 Wx = 0.981, and divergence asymmetry Θ_y / Θ_x = 1.004. Additionally, the radiation power passing through a diaphragm d = 12 mm at a distance of 800 mm from the laser was measured. Its value was 22 W with an incident power on the diaphragm of 21 W.

To evaluate the degree of polarization of the radiation from the prototype laser, an uncoated zinc selenide plate and a laser power meter were used. The plate was placed in the path of the laser beam and tilted in the vertical plane at the Brewster angle of 67.4°. Radiation power measurements were conducted at 20% PWM. In this setup, radiation with vertical polarization passes completely through the plate without reflection. Radiation with horizontal polarization was divided by the plate into two parts. One part passed through the plate, while the other part was reflected by the plate. It is shown that the laser radiation is elliptically polarized with a predominance of vertical polarization.

These experimental results confirm the preliminary estimates, except for the level of laser radiation power. This is due to additional losses in the *Z* -shaped discharge channel-waveguide due to insufficient quality of its inner surface treatment. To reduce losses, special milling cutters and aluminum oxide coating applied by spraying methods can be used.

6. CONCLUSION

The design features and technological modes at all stages of manufacturing a new generation of CO_2 -laser with transverse RF-excitation are proposed and justified.

Based on patent analysis and 3D design methods, the development and manufacturing of a domestic small-sized all-metal waveguide CO_2 -laser with transverse RF-excitation using domestic aluminum profiles was carried out, exceeding foreign analogues in parameters.

3D-prototyping allowed the development of design and technological documentation for small-scale production of a new generation of modern all-metal products using domestic aluminum profiles (rolled products) in their design.

REFERENCES

1. *Witteman W.J.* The CO_2 Laser. Textbook 1987.
2. *Karlov N.V.* Lectures on Quantum Electronics. Textbook. Moscow: Nauka, 1983.
3. *Pogorelsky S.L.* RF Patent 2065238, 1996.
4. *Laakmann P.* USA Patent 4805182, 1989.
5. *Vitruc P., Broderick J.A.* USA Patent 5953360, 1999.
6. *Payurov A.Ya., Kyun V.V., Rumyantsev R.S., Stepanov V.A., Fedorov M.A.* // Proc. II All-Russian Scientific and Practical Conference " Actual Problems of Physics and Technology in Education, Science and Production". Ryazan: RSU named after S.A. Yesenin, 2020. P. 94.

7. *Payurov A.Ya., Kyun V.V., Rumyantsev R.S., Stepanov V.A., Fedorov M.A.* // Proceedings of the XXVIII Int. Conf. "Laser-Information Technologies in Medicine, Biology, Geoecology and Transport. 2020". Novorossiysk: NGPU, 2020. P. 18.
8. TU 6-06-20-88 Adhesive film PKS-171 2008.
9. *Petrova A.P.* Adhesive Materials. Handbook / Ed. by E.N. Kablov, S.V. Reznichenko. Moscow: "Rubber and Elastomers", 2002.
10. *Lazutin Yu.D., Suskin V.V., Shevchenko V.F.* Mechanical Engineering Technology: textbook / Ed. by Yu.M. Soldak. Ryazan: RGRTU, 2008.
11. *Rosebury F.* Handbook of electron tube and vacuum techniques. Massachusetts, 1964.

FIGURE CAPTIONS

Fig. 1. Variant of Z-shaped discharge structure.

Fig. 2. Assembled discharge structure 3D and housing (box).

Fig. 3. 3D model and 2D drawing of the liquid radiator.

Fig. 4. Flanges with alignment units (2D and 3D images)
of power transistors.

Fig. 5. 3D model of a high-frequency driver.

Fig. 6. Box with discharge structure.

Fig. 7. Sealed box with optical system.

Fig. 8. Direction of heat flow movement.

Fig. 9. Direction of heat flows during liquid cooling.

Fig. 10. Block diagram of experimental setup for measuring energy and spectral characteristics of laser radiation: *1* – laser, *2* – power supply, *3* – cooling system, *4* – attenuator, *5* – IMO-4S power meter, *6* – two-coordinate recorder, *7* – radiation beam power density distribution meter, *8* – radiation wavelength meter (PAS).

Fig. 11. Scheme for measuring radiation beam divergence [4]: *1* – laser, 1–1, 2–2 – cross-sections in which radiation beam diameters are measured, L_1 – distance to the first cross-section, ΔL – distance between two cross-sections.

Fig. 12. Scheme for measuring laser beam diameter by radial distribution of radiation density.

Fig. 13. Dependence of radiation power on PWM level.

Fig. 14. Dependence of radiation power on gas mixture pressure (PWM=100%).

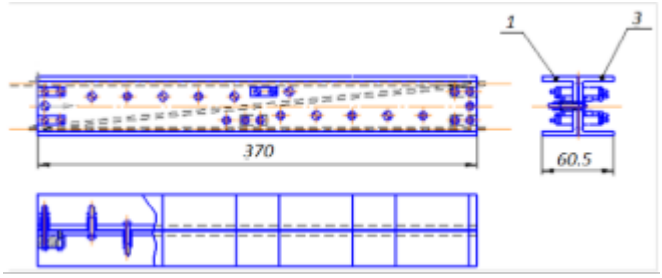

Fig. 1.

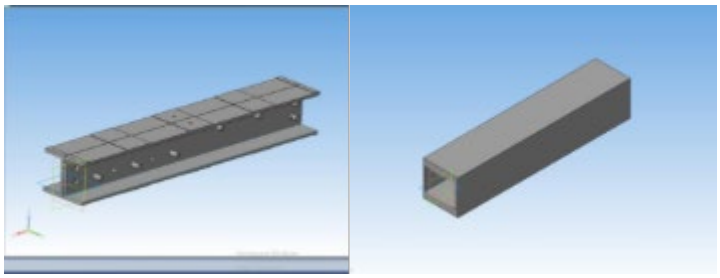

Fig. 2.

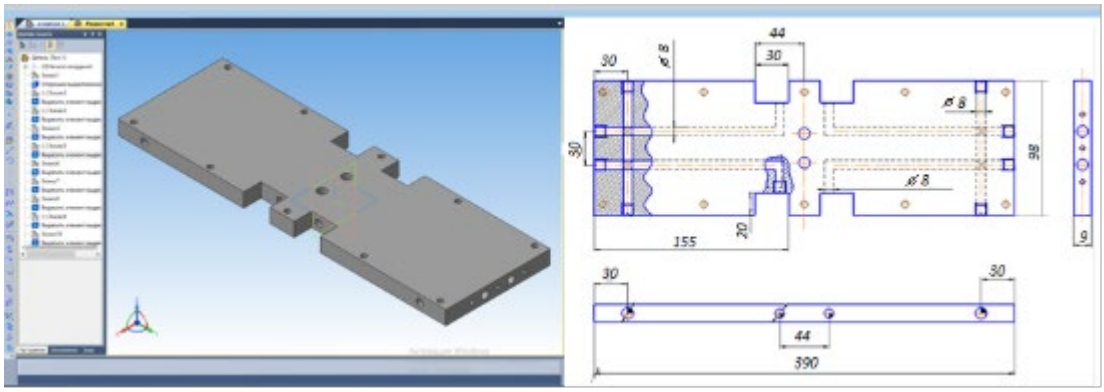

Fig. 3.

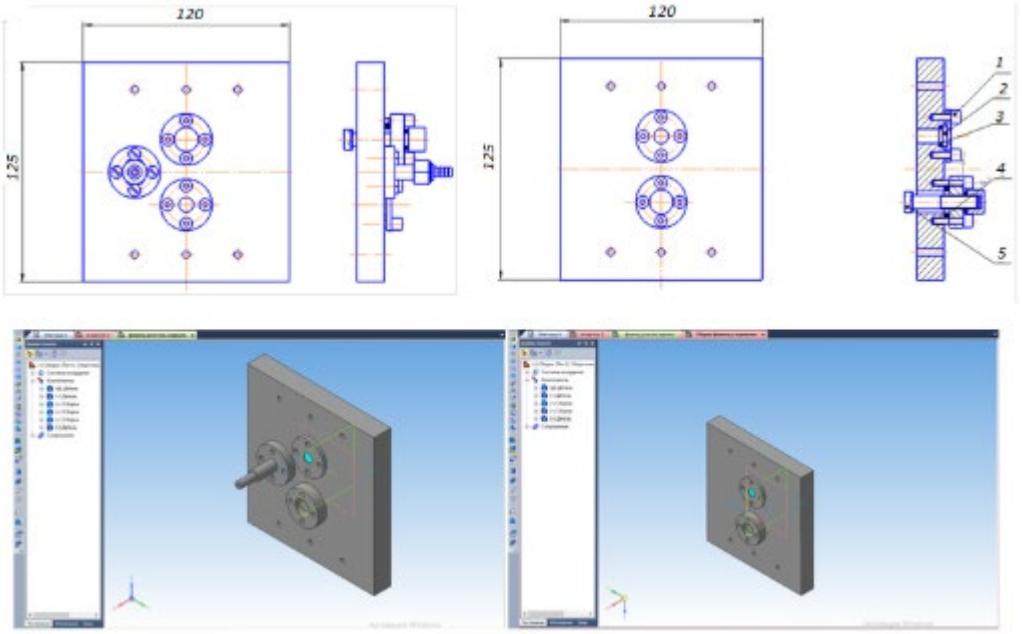

Fig. 4.

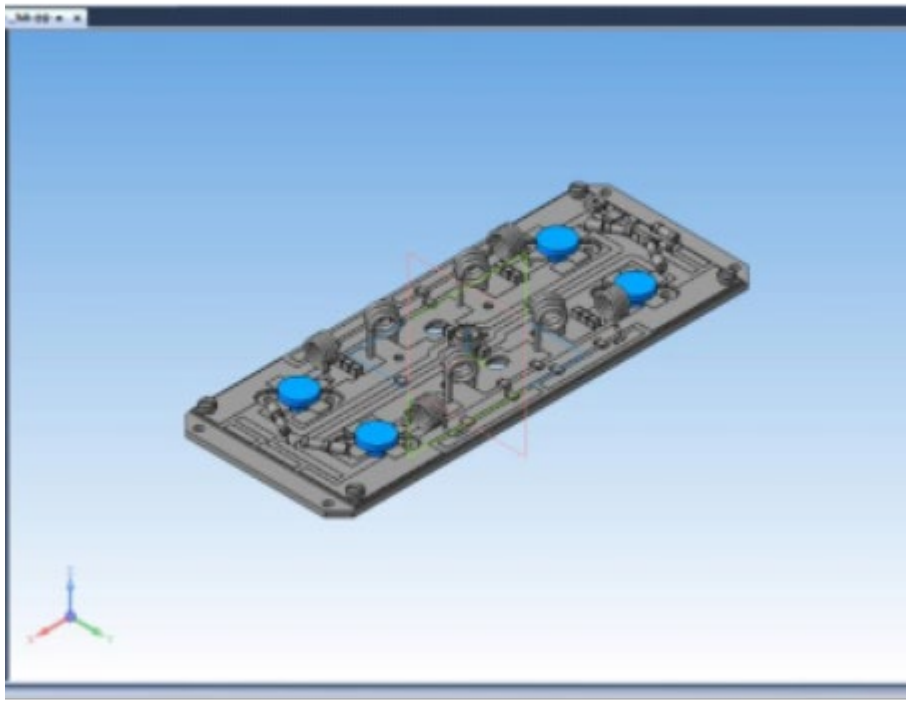

Fig. 5.

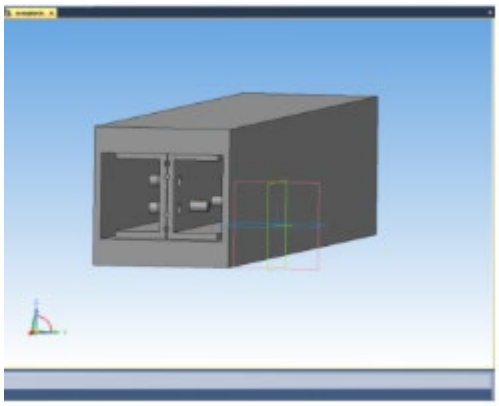

Fig. 6.

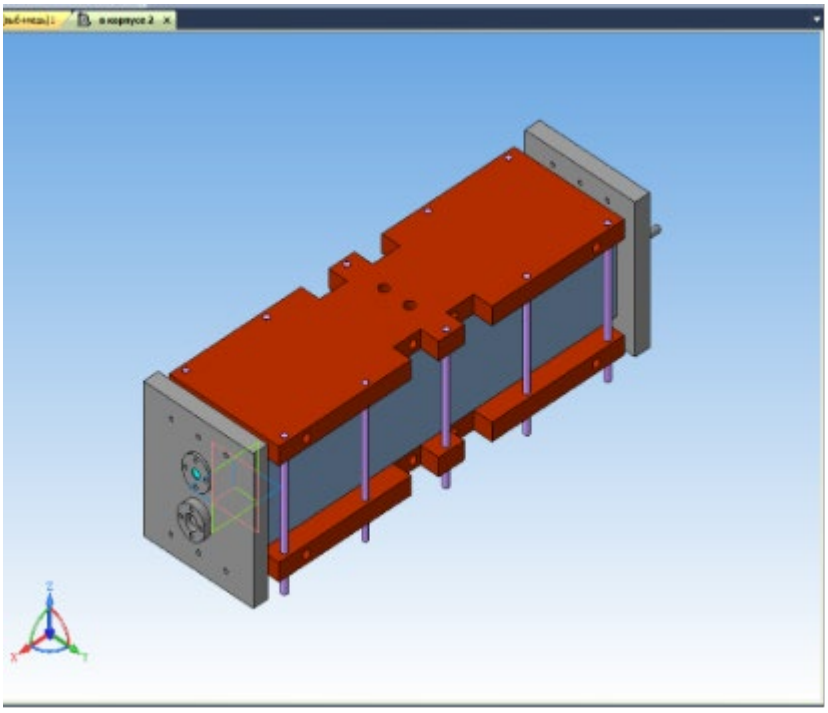

Fig. 7.

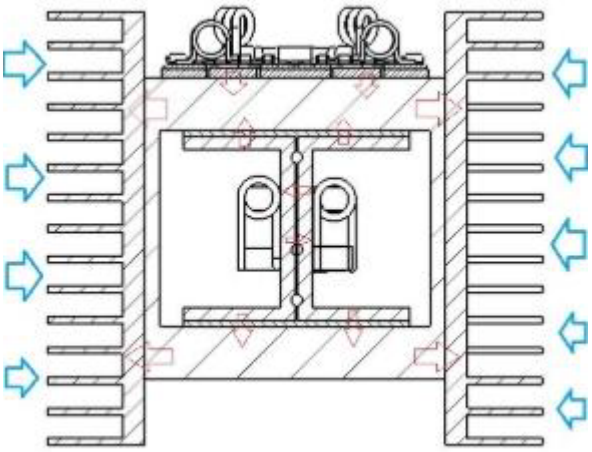

Fig. 8.

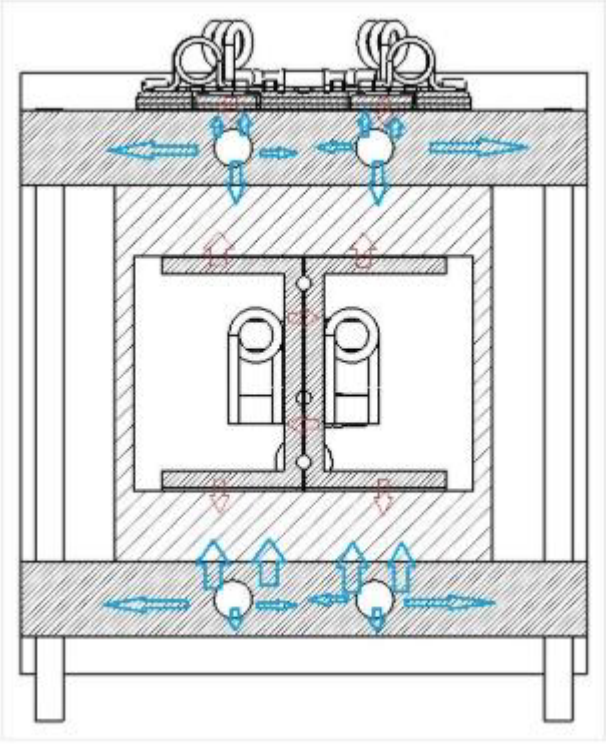

Fig. 9.

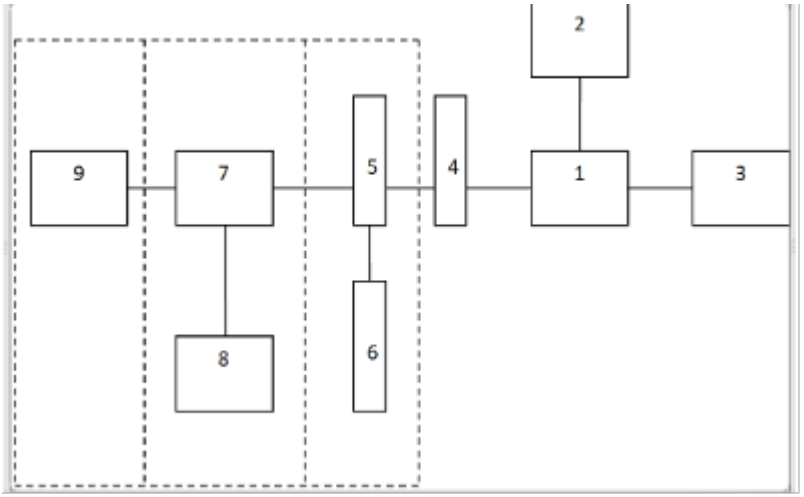

Fig. 10.

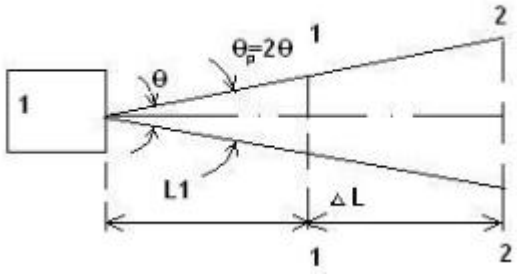

Fig. 11.

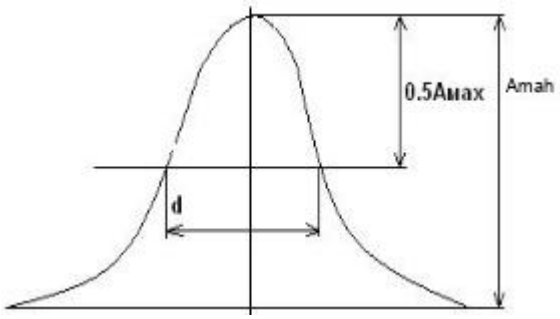

Fig. 12.

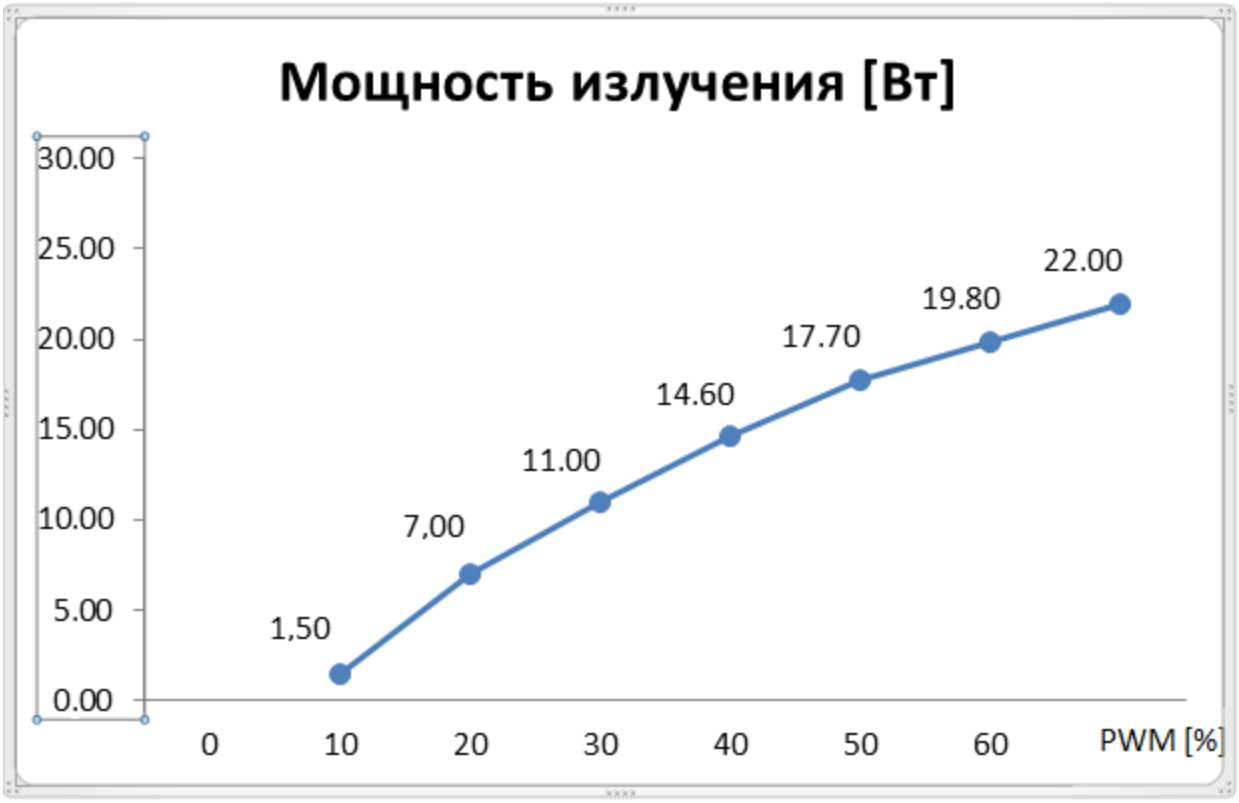
Мощность излучения [Вт]
30.00
25.00
20.00
15.00
10.00
5.00
0.00
1,50
7,00
11.00
14.60
17.70
19.80
22.00
0
10
20
30
40
50
60
PWM [%]

Fig. 13.

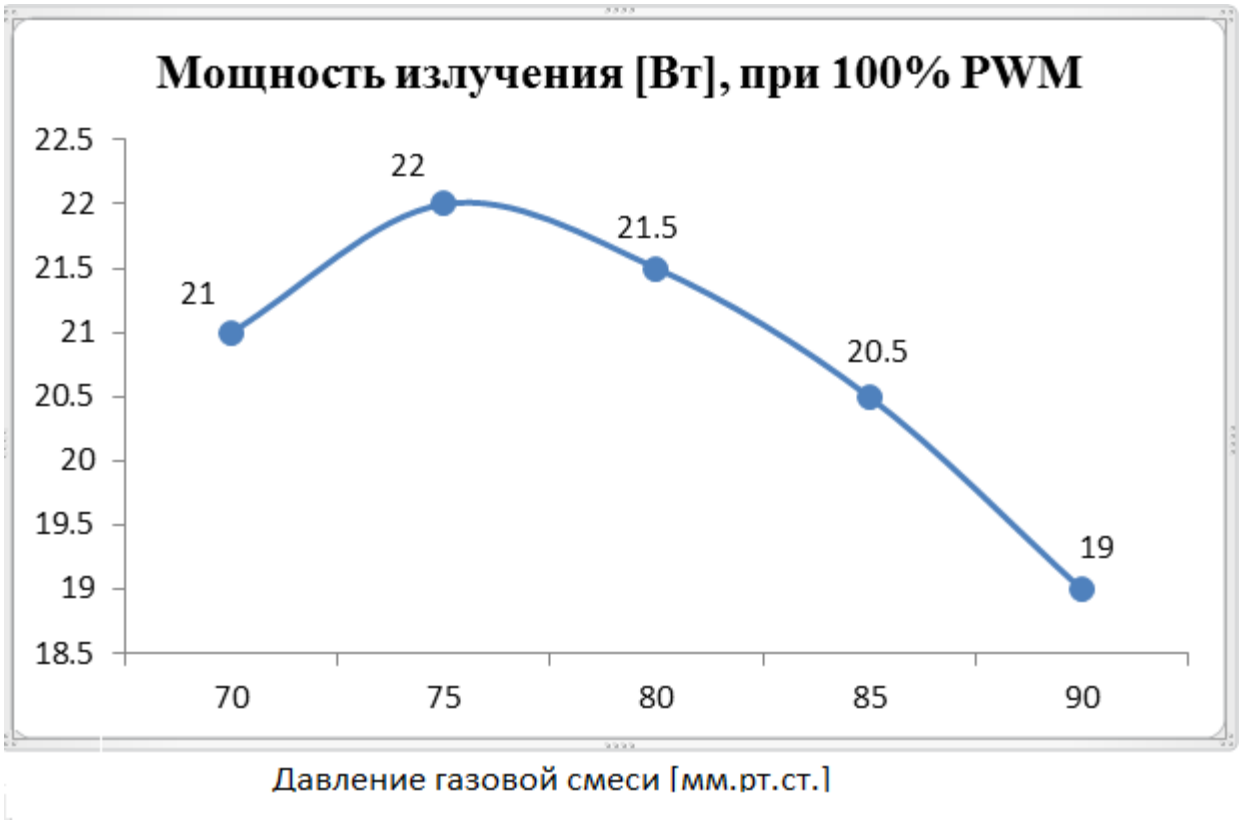
Мощность излучения [Вт], при 100% PWM
22.5
22
21.5
21
20.5
20
19.5
19
18.5
21
22
21.5
20.5
19
70
75
80
85
90
Давление газовой смеси [мм.рт.ст.]

Fig. 14.